2011 IEEE International Conference on Robotics and Automation
Shanghai International Conference Center
May 9-13, 2011, Shanghai, China

Continuum Model of Crossing Pedestrian Flows and Swarm Control Based on Temporal/Spatial Frequency

Ko Yamamoto and Masafumi Okada

Abstract— **In the densely-populated urban areas, pedestrian flows often cross each other and congestion occurs. It may cause discomfort feeling or pedestrian accidents. In order to reduce the congestion or the risk of accidents, it is required to control swarm flows of pedestrian. This paper proposes an implicit control method of the crossing pedestrian flows. Pedestrian flow is modeled with the continuum fluid model and its congestion degree is calculated as the fluid density. From a simulation of the crossing flows with the continuum model, it is verified that diagonal stripe pattern of the congestion degree emerges. Moreover, the authors propose an implicit control method to improve average flow velocity by moving guides. Focusing on periodic phenomenon of the crossing flows, we investigate the relationship between its temporal and spatial frequency and a periodic motion of guides. From this relationship, a control method based on the temporal and spatial frequency is proposed.**

I. Introduction

Congestion of pedestrian flows often occurs in the densely-populated urban areas. Moreover, pedestrian flows cross each other in the station, scramble crossing, museum, or event sites. For example, pedestrian flows with different destinations often cross around the ticket gate in the station, as shown in Fig. 1(a). It may cause discomfort feeling and pedestrian accidents. In order to reduce the congestion or risk of accidents, it is desired to make pedestrian flows smoother by guidance or navigation. For effective guidance, it is required to model and control pedestrian flows. Two types of model of pedestrian flows have been proposed: macroscopic model with fluid or continuum dynamics [1][2], and microscopic model with particle or homogeneous agent [3][4][5]. It is well known that a self-organization occurs in crossing pedestrian flows [2][6]. When flows cross vertically as shown in Fig. 1(b), diagonal stripe pattern emerges and the congestion degree of each flows varies in the crossing area. This phenomenon has been simulated with particle or homogeneous agent model [7][8].

On the other hand, for the navigation of pedestrians, methods to give commands to each individuals have been proposed [9]. However, all individuals need to carry a device to receive the commands. Therefore, it is difficult to apply this approach to crowded city with unspecified number of pedestrians. Although Narumi et al. [10] proposed a guidance system with moving image on the wall, their method is limited to direct guidance to individuals. In research fields of multi-robotics or multi-agent system, there are researches on *shepherding behaviors* [11][12]. This approach is indirect guidance of swarm, dealing with unspecified number of agents. Hereafter, we define *implicit control of swarm* as indirect control of macroscopic behavior with a limited number of commands. Okada and Homma [13] proposed a congestion reducing method with optimal location of partitions, which is also regarded as implicit control of swarm. They focused on a single flow, in which the congestion distribution converged to a steady state. In order to control pedestrian flows in the station or crossing, it is important to consider dynamical phenomenon of the congestion which emerges in the crossing pedestrian flows.

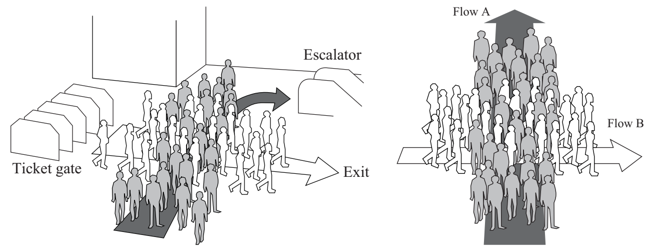

(a) (b)

Fig. 1. (a) Congestion in a station and (b) crossing pedestrian flows. When two pedestrian flows cross vertically, diagonal stripe pattern emerges.

In this paper, we propose modeling and control method of the crossing pedestrian flows. In a similar way to [2][13], we calculate the congestion degree as the density of continuum fluid based on the continuity equation of the compressive fluid. Moreover, an implicit control method to improve average flow velocity by moving guides is proposed. Focusing on periodic phenomenon of the crossing flows, we investigate the relationship between its temporal and spatial frequency and a periodic motion of guides. From this relationship, a control method based on the temporal and spatial frequency is proposed. We also apply the proposed method to the particle model by setting virtual density on each particles. We verify the validity of the method with simulations.

II. Macroscopic Model of Pedestrian Flow with Velocity Field

We consider pedestrian movement in two-dimensional space. In a similar way to [13], macroscopic behavior of pedestrian flow is modeled with a velocity field: velocity at

This research is supported by the *Research on Macro/Micro Modeling of Human Behavior in the Swarm and its Control* under the Core Research for Evolutional Science and Technology (CREST) Program (research area: Advanced Integrated Sensing Technologies), Japan Science and Technology Agency (JST).

The authors are with the Department of Mechanical Science and Engineering, Tokyo TECH, 2-12-1 Oookayama, Megutro-ku, 152-8552 Tokyo, Japan yamamoto@micro.mep.titech.ac.jp

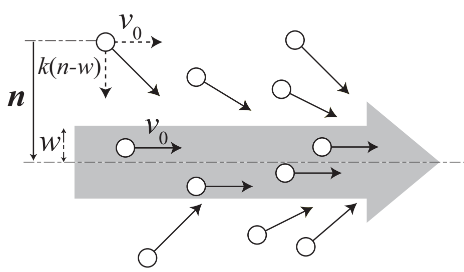

Fig. 2. Velocity vector field setting

position $\boldsymbol{x}$ is given by the following vector field $\boldsymbol{f}(\boldsymbol{x})$.

$$\boldsymbol{v} = \boldsymbol{f}(\boldsymbol{x}) \tag{1}$$

$$\boldsymbol{x} = \begin{bmatrix} x & y \end{bmatrix}^T \in \boldsymbol{R}^2 \tag{2}$$

Focusing on a pedestrian flow along a center line as shown in Fig. 2, $\boldsymbol{f}(\boldsymbol{x})$ is designed as follows:

$$\boldsymbol{f}(\boldsymbol{x}) = \begin{cases} v_0 \boldsymbol{d} & (\|\boldsymbol{n}\| \leq w) \\ v_0 \boldsymbol{d} + k(\|\boldsymbol{n}\| - w)\frac{\boldsymbol{n}}{\|\boldsymbol{n}\|} & (\|\boldsymbol{n}\| > w) \end{cases} \tag{3}$$

where $\boldsymbol{d}$ is the unit directional vector of the line, and $\boldsymbol{n}$ is the normal vector from the position $\boldsymbol{x}$ to the line. w and v_0 denote the width of the pedestrian flow and the reference velocity in the flow region. k is a magnitude of attracting effect to the flow.

In this section, we verify the diagonal stripe pattern formation in the crossing flows by modeling each pedestrian with a particle. We call this model *particle model*. Suppose that there are two pedestrian flows along x- and y-axes. Let the vector fields of the flows be $\boldsymbol{f}_A$ and $\boldsymbol{f}_B$, where their reference velocity is $v_0 = 1.0$ m/s. The velocity of a particle i along the vector field $\boldsymbol{f}_A$ is given as follows:

$$\boldsymbol{v}_i = \boldsymbol{f}_A(\boldsymbol{x}_i) - \sum_{i \neq j} s(\|\boldsymbol{r}_{ij}\|)\frac{\boldsymbol{r}_{ij}}{\|\boldsymbol{r}_{ij}\|} \tag{4}$$

$$\boldsymbol{r}_{ij} = \boldsymbol{x}_j - \boldsymbol{x}_i \tag{5}$$

where $\boldsymbol{x}_i$ and $\boldsymbol{v}_i$ are position and velocity of the particle i, respectively. This model is similar to the *Social Force Model* [3]. The first term in the right-side of (4) represents the attractive effect of the destination, and the second term represents a repulsive effect of the nearby particles (the particle i keeps a distance from nearby particles). $\boldsymbol{r}_{ij}$ is the relative position vector from the particle i to j. The repulsive effect is modeled with $s(r)$, a sigmoid function defined as follows:

$$s(r) = \frac{c}{1 + \exp\{a(r - b)\}} \tag{6}$$

where a, b and c are constant values. The velocity of particles along the vector field $\boldsymbol{f}_B$ is given in a similar way.

Then, we simulate the crossing flows which follow the vector field $\boldsymbol{f}_A$ and $\boldsymbol{f}_B$. Fig. 3 shows a snapshot of the simulation. We observed that a diagonal stripe pattern emerged after two flows have crossed. This result is consistent with the phenomenon mentioned in [6]. Therefore, the modeling of pedestrian flows with the velocity field is appropriate. However, it is difficult to evaluate the congestion degree

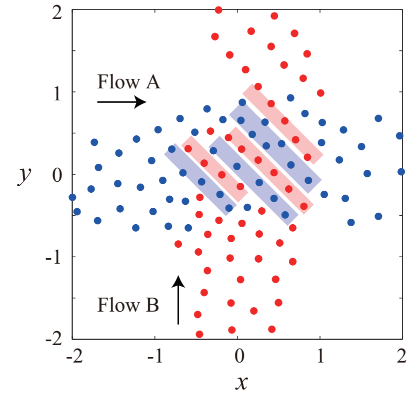

Fig. 3. Simulation of the crossing flows with the particle model

quantitatively. In the following section, we propose the continuum model of the crossing pedestrian flows.

III. Continuum Model of Crossing Pedestrian Flows

A. Continuum Model Based on Continuity Equation

Suppose that flow A and B follow the vector field $\boldsymbol{f}_A$ and $\boldsymbol{f}_B$, respectively. We quantify the congestion degree of flow A and B as ρ_A and ρ_B, the density of the continuum. Let the flow velocity be $\boldsymbol{v}_A = [v_A \; w_A]^T$ and $\boldsymbol{v}_B = [v_B \; w_B]^T$. In a similar way to [2][13], time variation of the flow density follows the following continuity equation.

$$\frac{\partial \rho_i}{\partial t} = -\rho_i\left(\frac{\partial v_i}{\partial x} + \frac{\partial w_i}{\partial y}\right) - \left(\frac{\partial \rho_i}{\partial x}v_i + \frac{\partial \rho_i}{\partial y}w_i\right) \quad (i = A, B) \tag{7}$$

Then, velocities of each continuum are given as follows:

$$\boldsymbol{v}_A = \boldsymbol{f}_A(\boldsymbol{x}) - \alpha\nabla\rho_A - \beta\nabla\rho_B \tag{8}$$

$$\boldsymbol{v}_B = \boldsymbol{f}_B(\boldsymbol{x}) - \alpha\nabla\rho_B - \beta\nabla\rho_A \tag{9}$$

where $\nabla\rho_i$ represents the following density gradient.

$$\nabla\rho_i = \begin{bmatrix} \frac{\partial \rho_i}{\partial x} & \frac{\partial \rho_i}{\partial y} \end{bmatrix}^T \tag{10}$$

The second and third terms in the right-hand side of (8) and (9) represent diffusion terms of each flow. α and β are their coefficients.

B. Simulation of Crossing Flows with Continuum Model

We simulate the density variation of the crossing flows based on the continuum model. Continuity equation (7) is calculated with the finite volume method. Assuming that pedestrians enter steadily, boundary conditions of the density is set as follows:

$$\begin{cases} \rho_A(\boldsymbol{x}, t) = \rho_{A0} & (x = -2, |y| \leq 0.5) \\ \rho_B(\boldsymbol{x}, t) = \rho_{B0} & (|x| \leq 0.5, y = -2) \end{cases} \tag{11}$$

We call ρ_{i0} input density. In this paper, we consider a case of $\rho_{A0} = \rho_{B0} = \rho_0$ for simplicity. Fig. 4 shows a simulation result of spatial distribution of density in steady state, setting $\rho_0 = 14$. In the figure, the blue color indicates $\rho_i = 0$, and

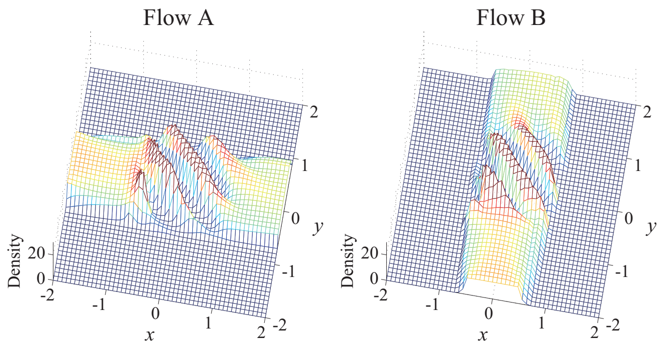

Fig. 4. Simulation result of spatial distribution of density in the crossing flows with the continuum model

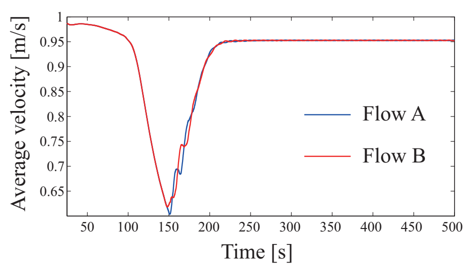

Fig. 5. Time variation of average velocity of the crossing flows

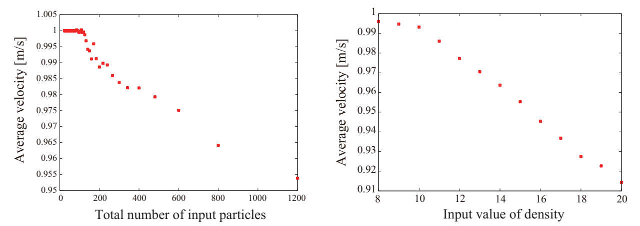

(a) Particle model (b) Continuum model

Fig. 6. Variation of the average velocity when the number of input is increased.

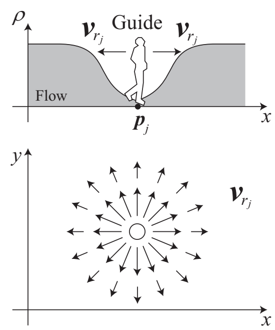

Fig. 7. Modeling of a guide and its effect to flows

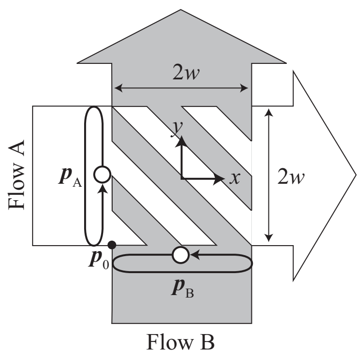

Fig. 8. Periodic motion of guides

the red color indicates the highest density. We observed that the diagonal stripe pattern emerged after the flows crossed.

In order to evaluate how smooth the pedestrian flows are, we define an average flow velocity. From actual velocity $\boldsymbol{v}_i(\boldsymbol{x}, t)$ at position $\boldsymbol{x}$, we extract the velocity element parallel to the original vector field $\boldsymbol{f}_i(\boldsymbol{x})$ as follows:

$$\hat{\boldsymbol{v}}_i = \boldsymbol{f}_i^{\#} \boldsymbol{v}_i \tag{12}$$

where $\boldsymbol{f}_i^{\#} = (\boldsymbol{f}_i^T \boldsymbol{f}_i)^{-1} \boldsymbol{f}_i^T$. Using $\hat{\boldsymbol{v}}_i$, we define the average velocity of time t as follows:

$$\bar{v}_i(t) = \frac{\int \rho_i \|\hat{\boldsymbol{v}}_i\| \, d\boldsymbol{x}}{\int \rho_i \, d\boldsymbol{x}} \quad (i = \mathrm{A}, \mathrm{B}) \tag{13}$$

The right-hand side of (13) implies proportionality of the total amount of flow rate to the density. Fig. 5 shows time variation of the average velocity in the crossing flows. The two flows collide at around 100s and the velocity declines rapidly. After that, the stripe pattern begins to emerge at 150s. After 200s, the stripe pattern propagates steadily and the velocity recovers.

C. Validation of Continuum Model

In order to verify the validity of the continuum model, we compared a variation of the average velocity of the particle model with the continuum model when the input number (or input density) was increased.

Firstly, in the particle model, we calculated the average velocity when the number of input particles in the total simulation time was increased. Fig. 6(a) shows the variation of the average velocity of the particles. When the number of input particles varied from 0 to 100, particles moved with the reference velocity v_0. As the total input number increased, the collision rate became higher and we observed that the average velocity decreases.

Next, in the continuum model, we calculated the average velocity of the crossing flows when the input density ρ_0 was increased. Fig. 6(b) shows the variation of the average velocity. When ρ_0 became larger than 11.5, the average velocity decreased in a similar way to the particle model. Therefore, it is shown that the property of flow velocity is well modeled with the continuum model.

IV. Control of Crossing Flows Based on Temporal/Spatial Frequency

A. Implicit Control of Swarm with Guides

We propose an implicit control method of the crossing flows by moving guides. Let the position of a guide be $\boldsymbol{p}_j$. Suppose that each flow is influenced by the repulsive velocity from the guide, as shown in Fig. 7. The repulsive velocity $\boldsymbol{v}_{r_j}$ at a position $\boldsymbol{x}$ defined as follows:

$$\boldsymbol{v}_{r_j} = -s(\|\boldsymbol{r}_j\|) \frac{\boldsymbol{r}_j}{\|\boldsymbol{r}_j\|} \tag{14}$$

where $\boldsymbol{r}_j = \boldsymbol{p}_j - \boldsymbol{x}$ is the relative position from the guide. Considering the repulsive effect, velocities of each fluid are determined as follows:

$$\boldsymbol{v}_A = \boldsymbol{f}_A(\boldsymbol{x}) - \alpha \nabla \rho_A - \beta \nabla \rho_B + \sum_j \boldsymbol{v}_{r_j} \tag{15}$$

$$\boldsymbol{v}_B = \boldsymbol{f}_B(\boldsymbol{x}) - \alpha \nabla \rho_B - \beta \nabla \rho_A + \sum_j \boldsymbol{v}_{r_j} \tag{16}$$

We move guides so as to improve the average flow velocity.

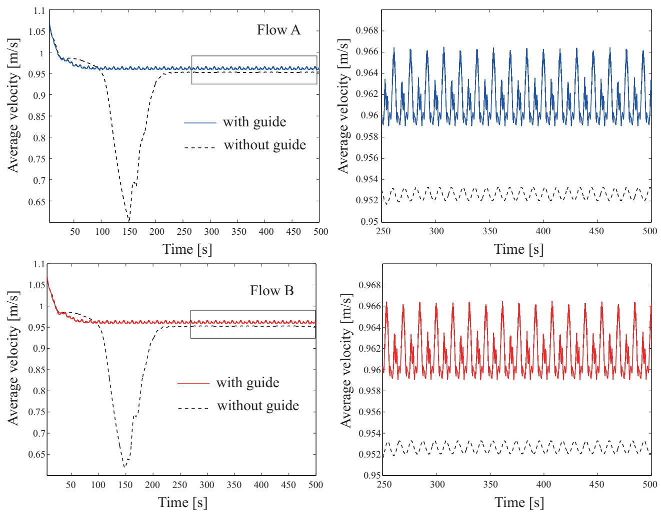

Fig. 9. Time variation of average velocity when guide people move periodically.

B. Temporal/Spatial Frequency Analysis of Crossing Flows

As shown in Sect. III, the density varies periodically in the crossing flows. In this section, we investigate variation of the average flow velocity when two guides are also moved periodically, as shown in Fig. 8. The positions of the two guides, $\boldsymbol{p}_A$ and $\boldsymbol{p}_B$, are given as follows:

$$\boldsymbol{p}_A = \boldsymbol{p}_0 + w\{1 - \cos(2\pi\omega_G t)\}\boldsymbol{d}_B \quad (17)$$

$$\boldsymbol{p}_B = \boldsymbol{p}_0 + w\{1 - \cos(2\pi\omega_G t + \pi)\}\boldsymbol{d}_A \quad (18)$$

where $\boldsymbol{p}_0$ is the intersection of the flows as shown in Fig. 8, w is the width of the flow, and ω_G is the motion frequency of the guides. $\boldsymbol{d}_A = [1\ 0]^T$ and $\boldsymbol{d}_B = [0\ 1]^T$ are directional vectors of each flow. We set the motion of the guides so that their phases are opposite. As shown in Fig. 8, the guides move vertically to the each flow in border lines of the crossing area.

Firstly, we simulated the density variation in the crossing flows with the guides, setting $\rho_0 = 14$ and $\omega_G = 0.065$Hz, for example. Fig. 9 shows simulation result of time variation of the average flow velocity. Rapid decrease of the velocity due to collision of the flows is prevented. The right columns of Fig. 9 show closeup of steady state between 250s and 500s. In both A and B, the average velocity is increased.

Next, we investigate relationship between the average velocity and guide frequency ω_G. The average velocity in the steady state of the crossing flows was simulated changing ω_G from 0.050 to 0.095Hz by 0.001Hz step size, where the input density is $\rho_0 = 14$. Fig. 10 shows the average velocity of the flow A. The average velocity is maximized when $\omega_{G0} = 0.062$Hz (indicated by the dashed line). If this optimal frequency ω_{G0} is found automatically, we can control the crossing flows so that the average velocity becomes large.

In order to find ω_{G0}, let us examine the characteristics of the crossing flows phenomenon when the guide frequency ω_G is lower or higher than ω_{G0}. In particular, we focus on temporal and spatial frequency of the crossing flows.

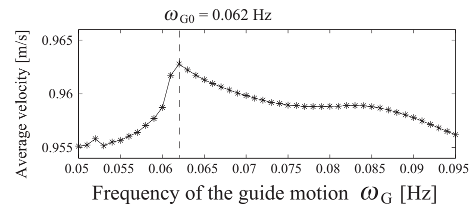

Fig. 10. Relationship between the frequency of guide motion ω_G and the average flow velocity, where the input density is $\rho_0 = 14$.

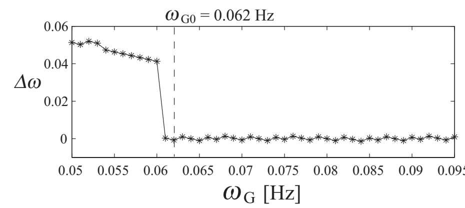

Fig. 11. Relationship between the frequency of guides ω_G and temporal frequency difference between the guide and the crossing flows $\Delta\omega$, where the input density is $\rho_0 = 14$.

Temporal frequency is computed by FFT analysis of time-series data of the density at a representative position, for example, the center position of the crossing area. Let the temporal frequency of the crossing flows be ω_F, and difference between ω_F and ω_G be $\Delta\omega$, namely,

$$\Delta\omega = \omega_F - \omega_G \quad (19)$$

Fig. 11 shows the relationship between ω_G and $\Delta\omega$. In the figure, the dashed line indicates the optimal frequency ω_{G0}. From this result, we can characterize the temporal frequency as follows:

- When ω_G is lower than ω_{G0}, $\Delta\omega$ decreases as ω_G increases.
- When ω_G is higher than ω_{G0}, $\Delta\omega$ is almost zero.

Next, let us examine the characteristics of the spatial frequency of the crossing flows. The inverse of the spatial frequency is equivalent to the width of the density stripe pattern, which is computed from spatial distribution of the density. Let the spatial frequency be ν_F. Fig. 12 shows relationship between ω_G and the spatial frequency ν_F. From this result, we can characterize the spatial frequency as follows:

- When ω_G is higher than ω_{G0}, ν_F increases as ω_G increases.

The above simulation results were calculated under the condition $\rho_0 = 14$. Results when the density input is given as

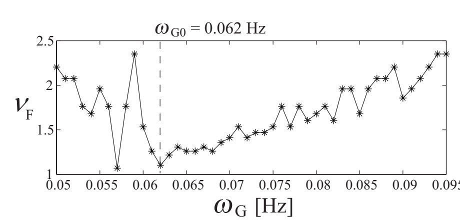

Fig. 12. Relationship between the frequency of guides ω_G and spatial frequency of the crossing flows ν, where the input density is $\rho_0 = 14$.

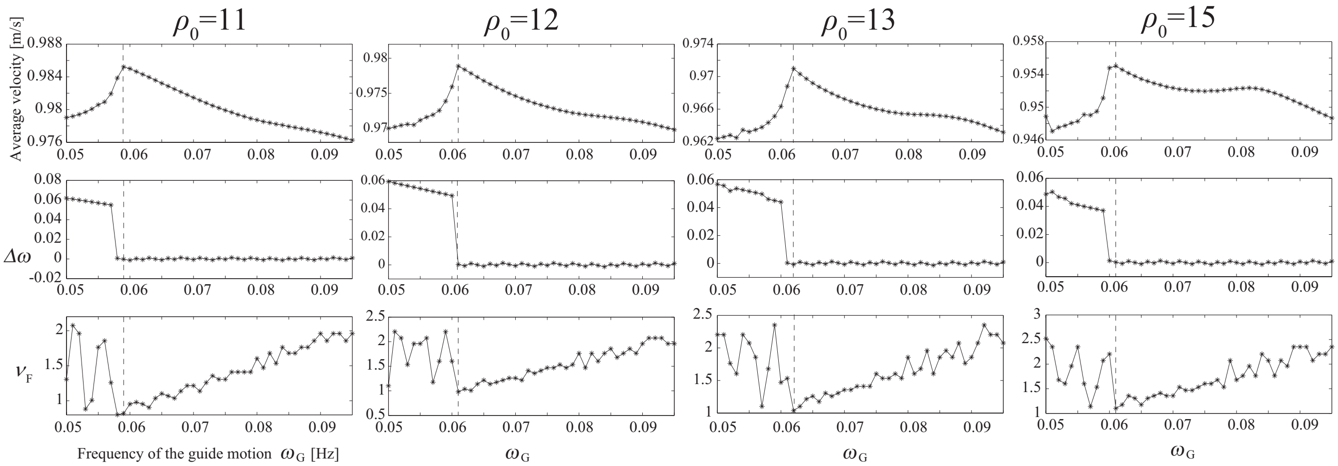

Fig. 13. Relationship between frequency of guides and average velocity of the flow A

$\rho_0 = 11, 12, 13, 15$ are shown in Fig. 13. The upper, middle and lower rows of Fig. 13 show the average velocity, $\Delta\omega$ and ν_F, respectively. These results are similar to those shown in Fig. 10, 11, 12.

C. Control Method Based on Temporal/Spatial Frequency

From the above discussion, it is possible to find the optimal guide frequency ω_{G0} by adjusting ω_G as follows:

1) In low-frequency area, ω_G is increased so that $\Delta\omega$ becomes zero.
2) In high-frequency area, ω_G is decreased so that ν_F becomes low.

We switch between these two strategies depending on if $\Delta\omega$ is equal to zero or not.

Let the guide frequency in the i-th period be ${}^i\omega_G$. From the temporal and spatial frequency of the crossing flows, ${}^i\omega_F$ and ${}^i\nu_F$, we determine the guide frequency in the next period ${}^{i+1}\omega_G$ as follows:

$$ {}^{i+1}\omega_G = \begin{cases} {}^i\omega_G + k_\omega \Delta\omega & (\Delta\omega \geq \Delta\omega_0) \\ {}^i\omega_G + k_\nu(\nu_0 - {}^i\nu_F) & (\Delta\omega < \Delta\omega_0) \end{cases} \tag{20} $$

where k_ω and k_ν are the gains of the temporal and spatial frequency, respectively. ν_0 is an offset value of the spatial frequency to prevent ω_G from changing rapidly near ω_{G0}. $\Delta\omega_0$ is a threshold of $\Delta\omega$.

D. Simulation of Crossing Flows Control

We simulated the density variation the crossing flows with the proposed control method. The density input was set as $\rho_0 = 14$, and the control parameters were set as follows: $k_\omega = 0.08$, $k_\nu = 0.001$, $\nu_0 = 1.0$. Fig. 14 shows the average velocities of the crossing flows, in which the right column shows closeup of the steady state between 250s and 500s. The average velocities increased by applying the proposed control method. Fig. 15 shows time variation of the guide frequency and the temporal frequency of the crossing flows. We observed that the guide frequency was adjusted so that $\Delta\omega$ becomes zero. Fig. 16 shows snapshots of the spatial distribution of the density. White poles indicate the position of the guides. We observed that the width of the stripe pattern increased. The attached video provides more detail.

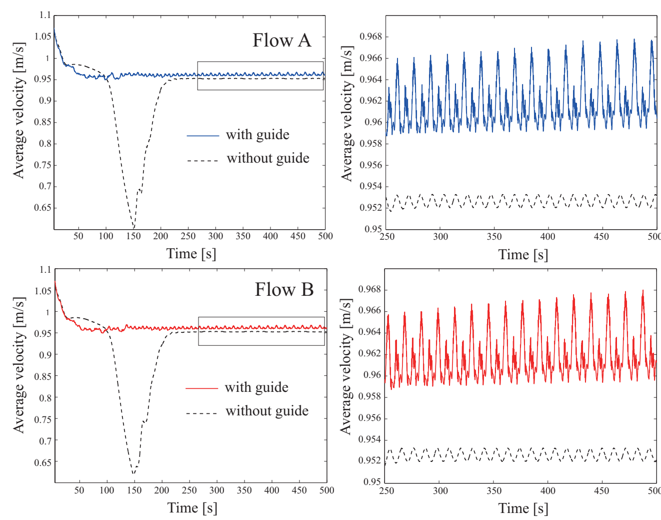

Fig. 14. Time variation of average velocity with proposed control method

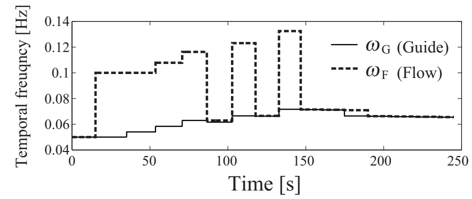

Fig. 15. Time variation of the guide frequency ω_G and the temporal frequency of the flow ω_F

V. Control of Crossing Flows with Particle Model

In order to apply the proposed control method to real crossing pedestrian flows, we need to calculate the density, which is a continuous quantity, from information of position and number of pedestrians, which are discrete quantity. We apply the proposed control method by calculating a virtual density from pedestrian position as follows:

$$ \hat{\rho}(\boldsymbol{x}) = \sum_i m_i W(\|\boldsymbol{r}_i\|, h) \tag{21} $$

where $\boldsymbol{x}_i$ and m_i are the position and virtual mass of a pedestrian, respectively. $\boldsymbol{r}_i = \boldsymbol{x}_i - \boldsymbol{x}$ is the relative position

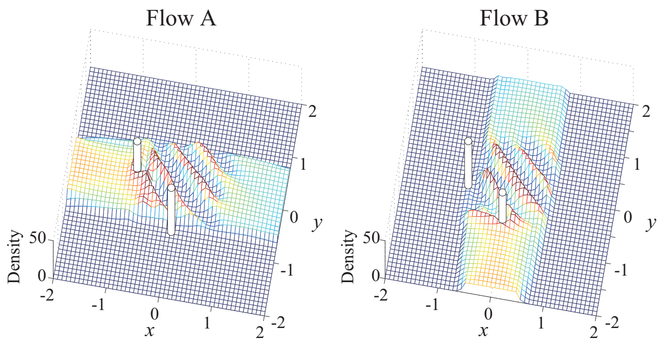

(a) $t = 50$s

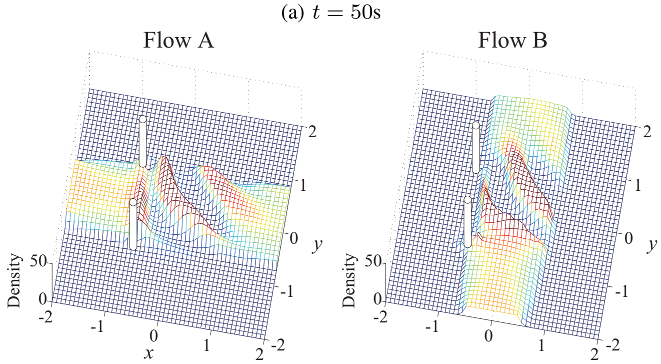

(b) $t = 250$s

Fig. 16. Simulation result of spatial distribution of density in the crossing flows with proposed control method

vector to the particle. $W(x,h)$ is the cubic kernel function defined by the following equations, which is often used in Smoothed Particle Hydrodynamics [14] in order to calculate the density.

$$W(x,h) = \begin{cases} \frac{10}{7\pi h^2}\left\{1 - \frac{3}{2}\left(\frac{x}{h}\right)^2 + \frac{3}{4}\left(\frac{x}{h}\right)^3\right\} & (0 \leq x < h) \\ \frac{5}{14\pi h^2}\left\{2 - \left(\frac{x}{h}\right)^3\right\} & (h \leq x < 2h) \\ 0 & (x \geq 2h) \end{cases} \tag{22}$$

We simulated the crossing flows with the proposed control method, assuming the particle model instead of actual pedestrian data. Setting $m_i = 1$ and $h = 0.15$, the virtual density and its temporal and spatial frequency were calculated. Fig. 17 shows a snapshot of the simulation. White circles indicate the guides. The attached video provides more detail. Fig. 18 shows time variation of the average flow velocity in the simulation. We observed that the velocity was improved by the proposed control method.

VI. Conclusion

In this paper, we proposed the continuum model of the crossing pedestrian flows and its implicit control method with guide motion. With the continuum model, we can evaluate the dynamical characteristics of the congestion. Then, we proposed a control method based on the temporal and spatial frequency of the crossing flows. Using this method, the average flow velocity was improved in both continuum model and particle model. The validity of the proposed method was verified by simulations.

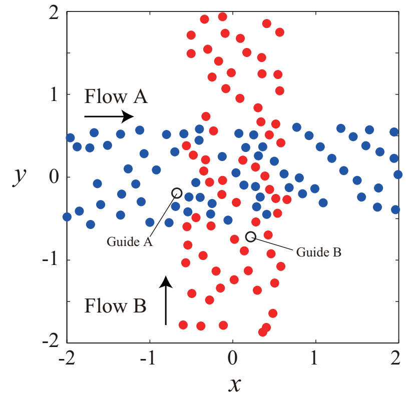

Fig. 17. Snapshot of the crossing flows by applying proposed control method to the particle model

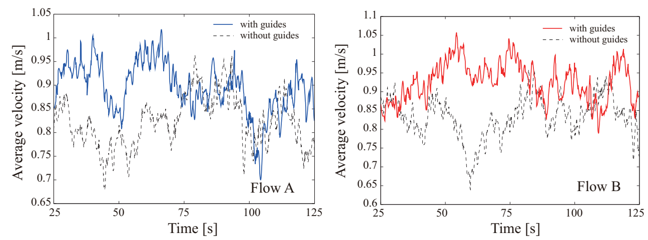

Fig. 18. Time variation of average velocity of the crossing flows by applying proposed control method to the particle model

References

[1] L. F. Henderson, "The Statistics of Crowd Fluids," *Nature*, vol. 229, pp. 381–383, 1971.

[2] R. L. Hughes, "A Continuum Theory for the Flow of Pedestrians," *Transportation Research Part B*, vol. 36, pp. 507–535, 2002.

[3] D. Helbing and P. Molnár, "Social force model for pedestrian dynamics," *Physical Review E*, vol. 51, no. 5, pp. 4282–4286, 1995.

[4] I. Karamouzas *et al.*, "A Predictive Collision Avoidance Model for Pedestrian Simulation," in *Motion in Games*, vol. 5884, 2009, pp. 41–52.

[5] S. J. Guy *et al.*, "PLEdestrians: A Least-Effort Approach to Crowd Simulation," in *Proc. of Eurographics/ ACM SIGGRAPH Symposium on Computer Animation*, 2002.

[6] K. Ando, H. Oto, and T. Aoki, "Forecasting the Flow of People (in Japanese)," *Railway Research Review*, vol. 45, no. 8, pp. 8–13, 1988.

[7] S. P. Hoogendoorn and P. H. Bovy, "Simulation of Pedestiran Flows by Optimal Control and Differential Games," *Optimal Control Applications and Methods*, vol. 24, no. 3, pp. 153–172, 2003.

[8] N. Pelechano *et al.*, "Controlling Individual Agents in High-Density Crowd Simulation," in *Proc. of Eurographics / ACM SIGGRAPH Symposium on Computer Animation*, 2007.

[9] K. Kurumatani, "Social Coordination with Architecture for Ubiquitous Agents: CONSORTS," in *Proc. of International Conference on Intelligent Agents, Web Technologies and Internet Commerce (IAWTIC2003)*, 2003.

[10] T. Narumi *et al.*, "Pedestrian Route Guidance System Using Moving Information Based on Personal Feature Extraction," in *Proc. of IEEE International Conference on Multisensor Fusion and Integration for Intelligent Systems*, 2008, pp. 94–99.

[11] R. Vaughan *et al.*, "Robot Control of Animal Flocks," in *Proc. of the 1998 IEEE ISIC/CIRA/ISAS Joint Conference*, 1998, pp. 277–282.

[12] J.-M. Lien *et al.*, "Shepherding Behaviors," in *Proc. of the 2004 IEEE International Conference on Robotics and Automation (ICRA2004)*, 2004, pp. 4159–4164.

[13] M. Okada and Y. Homma, "Amenity Design for Congestion Reduction based on Continuum Model of Swarm," in *Proc. of the 13th International Conference on Mechatronics Technology*, 2009.

[14] L. C. A. Pimenta *et al.*, "Control of swarms based on hydrodynamic models," in *Proc. of the 2008 IEEE International Conference on Robotics and Automation (ICRA2008)*, 2008, pp. 1948–1953.